

H. C. Burghard, Jr. and D. L. Davidson\*

## ABSTRACT

Recent developments in the applications of electron microscopy to the study of fracture surface topography have produced significant advances in fracture research. Clarification of fracture terminology and the formulation of microscopic fracture models have resulted. The recent contributions of topographic studies to basic fracture mechanisms are reviewed, and a proposed fracture classification in terminology consistent with this new work is included. Observations made on plastic fracture, cleavage, and fatigue crack propagation are included.

## INTRODUCTION

The technique of systematic examination of the topography of fracture surfaces, commonly referred to as fractography, has been recognized as a potentially valuable tool for the investigation of fracture mechanisms for several decades. However, early work in this field was severely restricted by the inherent limitations of optical microscopy. Such restrictions allow high-magnification observations only on extremely flat fracture surfaces. The application of the electron microscope, with its large depth of field and high resolving power, overcomes the limitations imposed by optical microscopy on the examination of the relatively rough surfaces commonly associated with fracture. This technique, labeled "electron fractography," has undergone extensive development in the past few years to the point where it is rapidly approaching the status of a standard metallographic procedure.

The interpretation of the fine scale features of fracture surfaces, in relation to the fracture mechanisms involved in their formation, is in some cases well established.<sup>(1, 2, 3)</sup> As a result, significant advances in the understanding of the mechanisms of fracture have been brought about by recent

---

\*H. C. Burghard, Jr. and D. L. Davidson, Southwest Research Institute, 8500 Culebra Road, San Antonio, Texas, U.S.A.

electron fractographic studies. In addition to these direct contributions to fracture research, advances in electron fractography have emphasized the need for a comprehensive and unambiguous framework of terminology for the description and discussion of fracture in general.

The objective of this paper is twofold. First, a classification of fracture processes and terminology, consistent with the observations of fine scale topographic features, is proposed. Secondly, the detailed observations are summarized to provide a current review of the relationship between fracture surface topography and the micro- and macro-mechanical aspects of fracture.

### FRACTURE CLASSIFICATION

As long as the direct observation of fracture surface topography was limited to examination at low magnifications, terms such as "ductile rupture," "brittle fracture," "intergranular," and "transgranular" were sufficient to describe and discuss fracture without confusion of terminology. However, the advent of electron fractography has emphasized the necessity for a more clearly established terminology. Attempts to completely describe fractures in terms of fine scale features and macroscopic characteristics can lead quickly to confusion. For example, features associated with microvoid growth and coalescence in tensile fractures of ductile materials were observed and recognized early in the development of electron fractography. The term "ductile rupture" was quickly applied to such a mechanism, consistent with the then current terminology. Further fractographic studies, however, resulted in observations of similar features in many very brittle fractures. Thus, adherence to the existing methods of classification required such paradoxical descriptions as "brittle fracture occurring by the ductile-rupture mechanism".

Examination of the factors involved in a fracture process leads to the conclusion that the specification of three characteristics is necessary for the complete description of the fracture; i. e., the basic mechanism involved, the relationship of the fracture path to the microstructure, and the macroscopic features of the fracture. These considerations, together with the fine scale topographic features observed in a large number of fractographic studies, suggest the following classification:

- (1) Basic mechanisms
  - (a) Plastic fracture
  - (b) Cleavage
  - (c) Fatigue

- (2) Fracture mode
  - (a) Transgranular
  - (b) Intergranular
- (3) Macroscopic characteristics
  - (a) Ductile
  - (b) Brittle

This classification satisfies the requirements previously outlined. It considers the three principal characteristics for describing a fracture, and provides subdivisions to include all necessary fracture terminology. This arrangement allows for modification of terminology as new information is gained.

The single feature common to every fracture is the creation of new surface. In the most fundamental sense, such new surface may be created in only two ways; by extensive crystallographic slip or by direct separation normal to specific crystallographic planes. The names given the numerous phenomena associated with these two mechanisms are "plastic fracture" and "cleavage," respectively. Plastic fracture is illustrated in the extreme by tensile fractures of high-purity metals which pull down to a point or chisel edge. The surface of the necked down region constitutes the major portion of the fracture surface. The fracture of ionic crystals along crystallographic planes is a familiar example of nearly perfect cleavage. Cleavage may also be induced in many body-centered-cubic and close-packed-hexagonal metals.

The fracture of materials under the influence of cyclic loading is a widely recognized class of fracture commonly described as fatigue. The mechanisms of propagation of a fatigue crack are not completely understood. Such crack growth, however, undoubtedly involves either plastic fracture or cleavage or a combination of both, depending upon the material and environmental conditions. Therefore, in the strictest sense, fatigue should not be considered as a basic fracture mechanism. However, until the mechanisms of fatigue are better understood, it will continue to be studied independently. In addition, fatigue failures occur under unique conditions and exhibit characteristic features. As a result, it is convenient to list fatigue as one of the basic fracture mechanisms.

The classification of fracture as to mode, concerns the relationship of the fracture path to the microstructure of the material. The terms "transgranular" and "intergranular" are sufficient for this purpose and are self-explanatory. It should be pointed out that each of these two modes of fracture may occur by any of the basic mechanisms.

The classification of a fracture as either ductile or brittle, according to the degree of macroscopic deformation involved, is necessary for the complete description of any particular fracture. The use of these two terms is well established and their definitions are widely accepted. It has been noted earlier that both brittle and ductile fractures may occur by a single mechanism. Thus, the use of these terms should be limited to describing the amount of macroscopic elongation or reduction of area accompanying the fracture. Care should be exercised to avoid the use of these two terms to either indicate or imply the basic mechanism of fracture.

It may be noted that this system of fracture classification makes no specific provision for the inclusion of such phenomena as stress corrosion cracking, and hydrogen embrittlement. These and other similar terms are in common use to describe specific fracture processes related to special environmental conditions or material history. Such phenomena are more properly regarded as fracture processes involving one or more of the basic mechanisms rather than as basic mechanisms themselves. Thus, each such process need not be specifically included. The classification does not prohibit the use of these terms, however, and indeed provides a more complete description of such fracture processes. In the event that further work establishes that any of these processes constitute unique mechanisms, such mechanisms may be included by a simple expansion of the subdivisions of the proposed classification.

## PLASTIC FRACTURE

The most common type of plastic fracture is the initiation, growth, and coalescence of microvoids. In such cases, microvoids are nucleated at preferred sites, grow under the influence of triaxial stresses and coalesce by localized internal necking. Such a mechanism creates a fracture surface passing through the center of a sheet of voids, resulting in numerous concave depressions in each fracture surface. The observation of such depressions, commonly referred to as "dimples," was first reported by Crussard<sup>(4)</sup> in 1959. Since that time, repeated observations of this characteristic feature have established that this mechanism occurs in many metallic materials and under a wide variety of conditions. The size and shape of the dimples formed by microvoid coalescence are strongly influenced by the state of stress prevailing during deformation, the environment, and by the microstructure of the material involved.

The influence of plastic strain conditions on the shape of dimples formed by microvoid coalescence has been investigated extensively by Brachem.<sup>(5)</sup> This work revealed three types of microvoid coalescence characterized by either equiaxed or elongated dimples. A schematic representation of each type and the corresponding fracture surface topography is given in Figure 1.

The growth of microvoids under the influence of a uniform principal tensile stress results in nearly spherical voids at the time of coalescence. The resulting fracture surface thus exhibits equiaxed dimples (Fig. 1a). When voids grow under the influence of a shear stress, they are elongated in the direction of shear, and the dimples in the resulting fracture surface are elongated and open at one end. These dimples point in the direction of shear on each fracture surface (Fig. 1b). The length-to-width ratio of elongated shear dimples is dependent upon the relative amounts of shear strain and normal strain occurring during the formation of the voids. The creation of a fracture surface by the propagation of a crack under nonuniform stress may be referred to as tearing. In such fractures, voids form and grow ahead of the crack and are intercepted by the crack front. This process also results in elongated open dimples; however, tear dimples are oriented so that the closed end points in the direction opposite to the direction of crack propagation (Fig. 1c). The length-to-width ratio of such dimples is a function of the ratio of the normal strain at the crack front to the average normal strain in the bulk material. Examples of each of the three types of dimpled structure are given in Figures 2, 3, 4 and 5.

Deformation processes related to plastic fracture have been studied in detail by Beachem and Meyn.<sup>(6)</sup> Four topographic features (glide plane decohesion, serpentine glide, ripples, and stretching) have been classified and correlated with various stages of plastic deformation of a surface. Glide plane decohesion is that mechanism by which slip occurs predominantly on one set of slip planes, causing an observable amount of new surface to be formed. This mechanism is rarely responsible for complete fracture but may be operative in localized regions. Serpentine glide is glide plane decohesion on several sets of planes simultaneously. This mechanism is thought to be formed by combinations of pencil or wavy slip, and cross slip, and is often found in polycrystalline materials where deformation in a given grain must accommodate the deformation of neighboring grains. Thus, slip is necessary on multiple planes, giving rise to slip steps which form an interwoven or plaited pattern. Further smoothing out of these steps (by plastic deformation) leads to the formation of ripples.

Subsequent plastic flow creates new surface on which the glide steps are so poorly delineated that the surface appears smooth and featureless. The term "stretching" is used to describe the processes which generate such surface areas. These topographic features are found on surfaces in which plastic flow has occurred, including surfaces created by microvoid coalescence. Beachem and Meyn present numerous examples of each of these features.

It should be noted that, in earlier work, the term glide plane decohesion has been used in conjunction with observed features which this subsequent work has shown to be the result of stretching. Glide plane decohesion is an important process in fracture, but care should be taken to use the term only in cases where the glide surfaces can be positively identified.

A fractograph illustrating ripples and stretching is shown in Figure 6. The stretching is indicated by separation of individual parts of fractured second-phase platelets. Ripples and stretched surfaces may also be noted in Figures 3 and 7.

The shape, size and size distribution of dimples are observed to be strongly influenced by microstructure. Evidence of the initiation of microvoids at second-phase particles or inclusions has been found in numerous investigations. In addition, it has been observed that localized regions of a fracture surface frequently exhibit dimples of markedly different size. To date, no extensive studies have been carried out for the specific purpose of correlating the features of microvoid coalescence with microstructure. Two observations have been made in a recent study of tensile fractures in an aluminum alloy in which the topographic features of base metal and welded joint fractures were examined. Fractures in weld deposits, where the microstructure consists of relatively large, uniformly distributed second-phase particles, were characterized by large, uniform dimples (Fig. 3). Early initiation of voids at the second-phase particles, followed by extensive growth, is indicated. However, in the age-hardened parent metal, where very few second-phase particles are found, typical fracture surfaces exhibited an extremely wide range of dimple sizes (Fig. 7). The larger dimples were consistently associated with the larger constituent particles, indicating that voids were initiated at these sites early in the deformation process. The smaller voids were apparently initiated later, and their coalescence constituted the final stage of fracture. These observations are consistent with the predictions of Gurland and Plateau.<sup>(7)</sup>

It should also be noted that in the large number of cases of microvoid coalescence observed to date, materials with fine-scale microstructures generally exhibit very small dimples, whereas, much larger dimples are usually observed in materials with coarser microstructures. This general observation is illustrated by comparison of Figures 2 and 3.

The extensive observations of fracture by microvoid coalescence in materials exhibiting a wide range of engineering ductility, and the extreme ductility exhibited by high-purity materials, suggest that the initiation and growth of voids governs ductility and toughness (excluding cases of fracture involving cleavage).

Edwards<sup>(8)</sup> has measured the depth of dimples in a large number of fractures exhibiting a wide range of macroscopic ductility. His results indicate an increase in the depth of dimples with increasing ductility. Further quantitative fractographic studies should establish a definite relationship between dimple size and shape and the macroscopic characteristics of fracture.

Numerous qualitative observations indicate that brittle fractures generally exhibit small dimples while larger dimples are characteristic of

more ductile fractures. Figure 8 is an example of a brittle fracture characterized by extremely small dimples. These dimples are in marked contrast to those seen in Figures 3 through 7. A brittle, intergranular fracture, also exhibiting small dimples, is shown in Figure 9.

## CLEAVAGE

Cleavage of a perfect crystal would be expected to produce a flat, featureless fracture surface coincident with a given crystallographic plane. Real crystals, however, are never perfect, and a cleavage crack, even if initiated as a single plane, is broken into a set of parallel cracks by imperfections. The propagation of a cleavage crack thus occurs by the simultaneous advance of a number of cracks on different planes. These cracks are joined by steps formed either by secondary cleavage or plastic fracture. Cleavage steps are generally observed to run together in the direction of local crack propagation, producing the familiar, characteristic "river patterns." An example of a typical cleavage facet is shown in Figure 10.

A comprehensive review of the nature and significance of the surface markings observed in cleavage fractures has been provided by Low.<sup>(9)</sup> In this review, it is pointed out that the most common origin of cleavage steps is that of screw dislocations intersecting the cleavage plane. The advance of a planar cleavage crack through a screw dislocation results in a shift of the level of the crack on each side of the dislocation. Low illustrates the dependence of the cleavage step formation on the density of screw dislocations by the behavior of cracks which propagated through sub-grain boundaries in Fe - 3% Si single crystals. The density of cleavage steps was observed to increase markedly as the crack passed through a twist boundary, while no change in the number of steps was evident when a crack crossed a pure tilt boundary. Similar observations have been reported for cleavage of LiF crystals,<sup>(10)</sup> and examples of the origin of steps at high-angle grain boundaries are given by Pelloux.<sup>(1)</sup>

The screw dislocations which give rise to cleavage steps may be attributed to several sources. They may be part of the network of grown-in dislocations present in any real crystal or they may be associated with low-angle twist boundaries. In addition, screw dislocations may be introduced by plastic deformation, either by prior deformation of the entire crystal or by glide occurring ahead of the advancing cleavage crack.

The generation of dislocations ahead of an advancing crack requires a velocity of propagation lower than a critical value.<sup>(11)</sup> In addition, the extent of glide ahead of a crack is strongly dependent on temperature. Since glide becomes easier with increasing temperature, it is conceivable that a critical temperature exists above which the energy necessary to form a cleavage crack (with its numerous steps) would exceed that necessary for

failure by plastic fracture. Low has illustrated this possibility by partially cleaving a zinc crystal at 78°K and completing the fracture at 300°K. The resulting fracture surface exhibited a high density of steps in the region corresponding to crack propagation at the higher temperature, while the low temperature fracture surface was relatively free of steps. The variation of the number and size of cleavage steps with temperature suggests the application of quantitative fractographic techniques to the study of cleavage fracture.

In polycrystalline aggregates, the local direction of crack propagation is often observed to vary from grain to grain. Individual cleavage facets may show directions of propagation nearly opposite to the macroscopic direction of crack propagation. Such variations are evident in Figures 10, 12 and 13. Figure 11 is an example of a cleavage fracture made up of a number of independent cleavage facets exhibiting numerous directions of local crack propagation. In this particular case, the cleavage facets are bounded by regions of limited plastic deformation, probably associated with grain boundaries.

In materials which undergo a ductile to brittle transition, fracture may occur by a combination of cleavage and plastic fracture. In general, the degree of plastic fracture increases with temperature through the transition zone. Examples of mixed cleavage and microvoid coalescence are shown in Figures 12 and 13.

Figure 11 and Figure 13 provide a comparison of the topography of impact fractures in irradiated and unirradiated steel tested under conditions resulting in nearly equal values of absorbed energy. It may be seen that the fracture surface of the irradiated material exhibits more extensive plastic fracture (in the form of microvoid coalescence) than that of the unirradiated material. This observation seems, at first, inconsistent with the general embrittlement brought about by irradiation. However, irradiation lowers the upper-shelf energy of the Charpy curve as well as shifting the ductile-brittle transition to higher temperatures. As a result, a given energy level on the Charpy curve of irradiated materials corresponds to more complete transition from cleavage to plastic fracture than a similar point on the curve of unirradiated materials. Thus, the observation of more extensive plastic fracture for irradiated materials is consistent with the shift of the Charpy curve. The cleavage steps observed on the irradiated specimens are generally less extensive than those of the unirradiated material, suggesting lower energy absorption by the cleavage portion of fracture in the irradiated specimens. This situation would allow more extensive plastic fracture at the same level of absorbed energy. In addition, it is possible that irradiation reduces the energy required to nucleate voids, thus lowering the energy absorbed by microvoid coalescence.

## FATIGUE

Cyclic propagation of a fatigue crack has been found to produce areas exhibiting a fracture surface topography which is characteristically different from that of other types of fracture. Usually some area of a fatigue fracture may be found which exhibits a series of parallel, though perhaps curved, regularly spaced, line-like fractures oriented normal to the direction of local crack propagation. These features, regardless of profile shape, are called striations. Striations were first observed by Zapffe and Worden,<sup>(12)</sup> Later, Forsyth and Ryder<sup>(13)</sup> showed that the striations represent successive lines along which the crack was arrested during each stress cycle. Even though one striation forms during each cycle, it has been found<sup>(3, 18)</sup> that local propagation rates may differ substantially from the macroscopically observable rate.

Striations, although characteristic of fatigue, are not always found on fatigue fracture surfaces. They are usually found on fracture surfaces created under plane strain conditions. Hertzberg<sup>(22)</sup> has observed regions of tear dimples in plane stress fatigue failures, and has concluded that striations are not likely to form under plane stress conditions. The presence of striations, then, is a clear case for the existence of fatigue, while their absence cannot be construed to indicate the absence of fatigue. Care must be taken when identifying fatigue striations that they are not confused with other features, such as Wallner's lines,<sup>(19, 27)</sup> interfacial cleavage and serpentine glide.

In general, face-centered-cubic and close-packed-hexagonal metals exhibit more clearly defined striations than do the body-centered-cubic metals. Presuming that slip ahead of an advancing crack influences its propagation characteristics, then the large number of possible slip planes in body-centered-cubic metals could result in less well defined slip than the close-packed metals which slip, except under unusual circumstances, only on close-packed planes. Due to the large number of orientations available in polycrystalline materials, a crystallite containing fatigue striations may usually be found somewhere on a fatigue fracture surface.

McEvily and Boettner<sup>(20)</sup> have observed that, in general, low stacking fault energy materials exhibit well defined striations, while those of high stacking fault energy do not. Frost<sup>(21)</sup> also found crack propagation rate to be dependent on stacking fault energy. By comparison, the close-packed metals have much lower stacking fault energies than do the body-centered-cubic metals. Apparently, the ease of cross-slip in high stacking fault energy materials causes striations to be ill-defined. In contrast to the beautifully formed striations seen in aluminum by Forsyth<sup>(15)</sup> and Pelloux,<sup>(22)</sup> Figure 14 is an example of how poorly formed they may be in a high-strength steel. Crussard, et al,<sup>(4)</sup> have shown that, in mild steel,

increasing prestrain causes striations to become more ill-defined to the point where they cannot be distinguished after 15 percent prestrain.

The shape, length and general characteristics of fatigue striations have been studied in some detail, (22, 26) and it appears that there are many factors which influence their shape. The orientation of the crystallite through which the crack is propagating, its previous strain history, the stress state and magnitude, and the shape and frequency of the loading all appear to influence striation characteristics. Of the several detailed mechanistic studies made of fatigue, the early studies of Forsyth and Ryder<sup>(14)</sup> and Laird and Smith, (23) and the later studies of Forsyth,<sup>(15)</sup> Stubbington, (16) Schijve, (17) and Hertzberg<sup>(22)</sup> offer the best available information contributing to a basic understanding of fatigue crack propagation. In all these investigations, the study of the striation profile shape was found to be a key factor in determination of how the striations were formed.

Although all the studies were made on face-centered-cubic metals, Forsyth and Ryder, Forsyth, Stubbington, and Schijve studied low-stress fatigue, while Laird and Smith studied high-stress fatigue. Laird and Smith state that because fatigue striations are formed during both high- and low-stress fatigue, the mechanism of their formation is very likely the same. Schijve essentially supports this view, although he hypothesizes that the actual dislocation mechanisms associated with crack propagation in each case may be different. Forsyth, Schijve and Stubbington have shown marked differences in striation profile from that observed by Laird and Smith. Hertzberg studied both low and high stress fatigue, and concluded that the mechanisms are the same in both cases.

Laird and Smith utilized the light microscope to determine profile shape of the striations they observed. Limited use was also made of an electron scanning microscope to study the fracture surface, but their main contribution was the ingenious method used to stop the fatigue crack at different portions of the cycle so that the steps in the growth of a striation could be examined. From their observations, they propose a sequence for crack extension in a plastic material which is crystallographically independent (see Fig. 15). Striations of this same profile have also been seen in other aluminum alloys. (1, 3)

According to Williams<sup>(24)</sup> applications of a tensile load to an elastic body containing a sharp crack under plane stress conditions results in maximum tensile stress along radials which are  $\pm 60^\circ$  from the crack plane. The value of this stress is approximately 1.3 times the maximum stress to be found elsewhere and is directed perpendicular to the crack plane (see Fig. 16). The maximum shear stress and the maximum energy of distortion occur at an angle of  $\pm 70^\circ$ . Thus, it is reasonable to believe that initial yielding, and subsequent fracture, will take place along a plane  $\pm 60$  to  $70^\circ$  to the plane of the crack. However, yielding or fracture along one of these planes will

change the conditions under which the original analysis was made to something more closely akin to Williams' analysis of a crack in antisymmetric loading. In this case, the maximum stresses and maximum distortion energy occur on the main crack plane. Thus, after initial yielding, deformation may be shifted back to the area just ahead of the main crack. The compression portion of the cycle then presses the crack shut, further sharpening it. From Williams' analysis, it appears that roughly equal values of shear and tensile stress act on a plane  $\pm 60^\circ$  to  $70^\circ$  from the main crack plane. Thus, both plastic fracture and cleavage are possible on that plane. The mechanism of crack propagation in a particular fracture will probably depend on material characteristics and crystal orientation.

Similar, although more detailed, calculations have been carried out by Schijve<sup>(17)</sup> on the distribution of shear stresses around a crack loaded in tension and pure shear, both for plane stress and plane strain conditions. For all cases, his calculations show essentially the same result as Williams' analysis. Schijve also investigated the distribution of shear stress around the crack as the angle between the tensile axis and the crack plane was varied between  $90^\circ$  and  $45^\circ$ . As might be expected, there is a tendency toward increasing shear stress in line with the crack as its direction changes toward the tensile axis. Thus, if shear stress controls crack propagation, the crack is likely to propagate in a path other than at right angles to the tensile axis.

Forsyth observed and described two types of fatigue striations. One was characterized by relatively flat facets marked periodically by sharp grooves. River patterns were frequently observed on the facet surfaces, and secondary cracking was prevalent. These topographical features suggest that this type of striation is formed predominantly by cleavage. Forsyth observed that these characteristics prevailed where fatigue occurred in a corrosive environment. The other type striations Forsyth observed had rounded bottoms, relatively flat sides, sharp peaks at the top, and appear to be at least partially formed by plastic fracture. Forsyth proposed a mechanism whereby these striations are formed in two steps during the tension part of the cycle. The details of his mechanism are not clear, but he apparently proposes that the first part of the striation is formed by separation along a crystallographic plane, while the second part is due to cross-slip of dislocations.

Hertzberg has made a detailed study of striation formation and has shown that in tension-tension loading, half of the striation was formed during the loading part of the cycle, and half the striation was formed during unloading. He has proposed a mechanism of striation formation (for face-centered cubic metals) based on slip on alternate specific crystallographic planes.

Stubbington also observed and described two types of striations. He fatigued aluminum alloys in air and a dilute salt solution at low stresses. From his observations, he concluded that cleavage was associated with both types of striations, and that the corrodent acted to increase the portion of the striation formed by cleavage. A profile section through the advancing crack shows a clearly defined saw tooth pattern, although there is no indication on either side of the striation as to its mechanism of formation. Stubbington states that, in normal atmospheric environments, approximately half the striation is formed by cleavage and half by plastic fracture. Like Forsyth, Stubbington presents a mechanism in which both parts of the striation are formed during the tension part of the cycle. He postulates that the compression part of the cycle conditions the material immediately ahead of the crack root for cleavage during the subsequent tensile cycle.

Stubbington shows a profile through striations formed predominantly by cleavage, revealing intense slip lines on one of the fracture surfaces at each crack arrest point. The striations thus formed are very similar to those observed by Forsyth. Although some detailed high-resolution photographs would have greatly strengthened Stubbington's conclusions on striation formation in air, he has presented in a very clear manner many details of his observations on the specimens fatigued in a corrosive atmosphere. Most significantly, he has shown that both fracture surfaces match in a peak to valley manner in all the profiles presented.

Schijve fatigued pure aluminum and aluminum alloys in low stress fatigue. The experimental portion of this paper suffers from the lack of high-resolution fractographs. In low magnification profiles of the fracture path, slip lines were observed to be associated with most of the crack profiles shown. This leads Schijve to the conclusion that plastic fracture is very closely associated with formation of the whole striation. He postulates two dislocation mechanisms based on this observed slip. The mechanisms are quite detailed, but depend essentially on the generation of new dislocations at the crack tip in one case, and an absorption of dislocations at the crack tip in the other. Many other aspects of fatigue fracture are also covered in this rather thorough review.

It is apparent from the investigations made so far that a detailed knowledge of the formation of fatigue striations is necessary for a complete understanding of the mechanisms of crack propagation. Any proposed mechanism must be consistent with observed profile configurations and the matching characteristics of mating fracture surfaces.

Figure 17 schematically represents three basic striation profile configurations consistent with those observed to date. The emphasis of this figure is on how the surfaces of the fractured parts match together as well as profile shape. Type I striations were observed by Laird and Smith with their sectioning technique, and probably result chiefly from plastic fracture.

Type II striations could be the result of either plastic fracture or cleavage, or both, and have been observed by Forsyth and Ryder<sup>(14)</sup> (a modification of Type IIb or IIc), Forsyth, Stubbington, and Pelloux.<sup>(18)</sup> Details of the striations observed by Forsyth and Ryder are presented in a schematic form only, peak to peak, with cleavage in between. Forsyth shows a fractograph of Type IIa or IIb striations and a cross section of Type IIc striations. The mechanism he postulates is for the Type IIa or IIb striation, although it is not clear which type of matching his mechanism explains. Stubbington, on the other hand, has clearly observed Type IIa striations.

It will be noted that the void growth mechanism proposed by Forsyth and Ryder<sup>(14)</sup> has not been included. It is generally accepted that this mechanism is unlikely, due to the improbability of the repeated nucleation and growth of a long thin (sausage-shaped) void the full length of and just ahead of the crack front. If the process of void growth and coalescence with the main crack is responsible for crack propagation, the striations should consist of rows of small tear dimples rather than the smooth sides that are observed.

Forsyth proposed a crack propagation model which would produce a profile similar to Type III to explain his observations of striations formed predominantly by cleavage. This model considers the major portion of propagation as cleavage on (100)-planes, followed by some form of plastic fracture, which results in the peak and valley features separating the cleavage facets. Some features observed in a cross section of such a crack support this type of matching; however, the evidence is not conclusive. Stubbington's observations provide further support of the Type III profile. It thus appears that striation formation under corrosive conditions in aluminum and its dilute alloys is rather well understood despite an inexact knowledge of details of the mechanisms of formation.

Combinations of plastic fracture, as exemplified by dimples, and fatigue striations have been observed in high-stress fatigue of austenitic steel. Figure 18 shows such a fracture surface near the origin of the crack. Well-formed isolated voids have apparently developed in the region ahead of the crack front. Interaction between individual voids and the advancing crack front is evident and appears similar to that occurring between second-phase particles and an advancing fatigue crack.<sup>(3, 22)</sup> The crack in all cases appears to accelerate in the vicinity of a void, as would be expected from the stress conditions associated with this geometric condition. Nearer the termination of the same fracture, Figure 19, the dimples become larger and exhibit marked surface irregularities. This suggests that the voids have undergone extensive growth in a cyclic manner, although no fatigue striations, as such, are seen. The absence of tear dimples supports this suggestion. Figure 20 is another example of this phenomenon and is similar to observations made by Dahlberg.<sup>(25)</sup>

## CONCLUSIONS

The topographic features of plastic fracture have been thoroughly studied, and the processes of their formation are relatively well understood. For the further understanding of plastic fracture, a quantitative correlation of dimple size, shape, and size distribution to microstructure and environment should be established. The features characteristic of cleavage are equally well delineated and understood. A quantitative correlation of surface features with fracture energy would provide significant additional information. In contrast, fatigue is not nearly as well understood. Striations have been established as the topographic feature most generally associated with fatigue. The observations to date have established a firm basis for additional studies which should include further investigation of the fine scale surface features and surface matching characteristics. The phenomena of stress corrosion and hydrogen embrittlement need extensive systematic investigation, from which, it is hoped, a basic understanding will develop. The one thing that is seen from all the studies made to date is that the extensive application of detailed quantitative fractography is the next obvious development.

## REFERENCES

1. R. M. N. Pelloux, "The Analysis of Fracture Surfaces by Electron Microscopy," Report D1-82-0169-R1, Boeing Scientific Research Laboratories, Seattle, Washington, Dec. 1963.
2. C. D. Beachem, and R. M. N. Pelloux, Paper presented at ASTM Annual Meeting, June 1964.
3. V. Kerlins, A. Phillips, and B. V. Whiteson, "Electron Fractography Handbook," ML-TDR-64-416, Wright-Patterson AFB, Jan. 1965. (Prepared by Douglas Aircraft Co., Santa Monica, Calif.)
4. C. Crussard, J. Plateau, et al., Fracture, p. 524, John Wiley & Sons, Inc., 1959.
5. C. D. Beachem, Trans. ASM, 56, p. 318, 1963.
6. C. D. Beachem, and D. A. Meyn, NRL Memorandum Report 1547, U. S. Naval Research Laboratory, Washington, D. C., June 1964.
7. J. Gurland and J. Plateau, Trans. ASM, 56, p. 442, 1963.
8. A. J. Edwards, Report of NRL Progress, p. 19, U. S. Naval Research Laboratory, Washington, D. C., Nov. 1963.

9. J. R. Low, Jr., Fracture, p. 68, John Wiley & Sons, Inc., 1959.
10. J. J. Gilman, Trans. AIME, 212, p. 310, 1958.
11. J. J. Gilman, Trans. AIME, 209, p. 449, 1957.
12. C. A. Zapffe, and C. O. Worden, Trans. ASM, 43, p. 958, 1951.
13. P. J. E. Forsyth, and D. A. Ryder, Aircraft Engineering, 32, p. 96, 1960.
14. P. J. E. Forsyth, and D. A. Ryder, Metallurgia, 63, p. 117, March 1961.
15. P. J. E. Forsyth, Acta Metallurgica, 11, p. 703, July 1963.
16. C. A. Stubbington, Metallurgia, 68, p. 109, Sept. 1963.
17. J. Schijve, "Analysis of the Fatigue Phenomenon in Aluminum Alloys," NLR-TR M.2122, National Aero- and Astronautical Research Institute, Amsterdam, Netherlands, April 1964.
18. R. M. N. Pelloux, Trans. ASM, 57, p. 511, June 1964.
19. H. Schardin, Fracture, p. 297, John Wiley & Sons, Inc., 1959.
20. A. J. McEvily, and R. C. Boettner, Fracture of Solids, p. 383, John Wiley & Sons, Inc., 1963.
21. N. E. Frost, Proc. Inst. Mech. Engrs., 1, p. 151, 1959.
22. R. W. Hertzberg, Ph.D Thesis, Lehigh University, 1965.
23. C. Laird, and G. C. Smith, Phil. Mag. (8), 7, p. 847, 1962.
24. M. L. Williams, J. Appl. Mech., 24, p. 109, March 1957.
25. E. P. Dahlberg, Trans. ASM, 58, p. 46, 1965.
26. G. Jacoby, Exper. Mech., 5, p. 65, March 1965.
27. H. Wallner, Z. Physik, 114, p. 368, 1939.



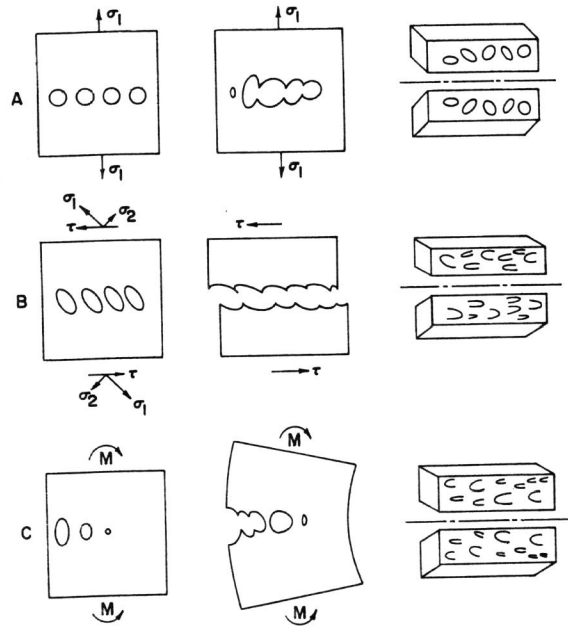


FIGURE 1. SCHEMATIC REPRESENTATION OF VOID GROWTH AND COALESCENCE IN PLASTIC FRACTURE. (After Beachem<sup>3</sup>).

- (a) Formation of equiaxed dimples under influence of uniform plastic strain in direction of applied stress.
- (b) Formation of elongated dimples under influence of shear strain. Dimples point in direction of shear on each surface.
- (c) Formation of elongated dimples under influence of nonuniform plastic strain in direction of applied stress. Dimples point in direction opposite to the direction of crack propagation.



FIGURE 3. TENSILE FRACTURE OF Al-4.5% Cu (Alloy 2219) WELDMENT. Large, uniform, equiaxed dimples formed by microvoid coalescence. Arrows indicate origin of voids at second-phase platelets.

Two-Stage, Plastic-Carbon Replica 5000X

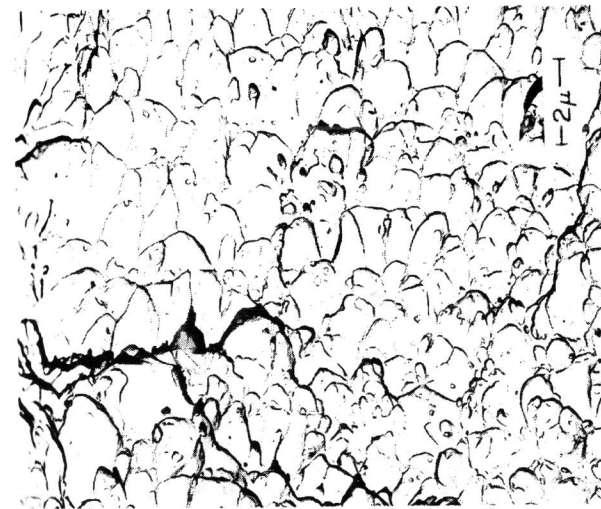


FIGURE 2. TENSILE FRACTURE OF HY-80 STEEL. Small, uniform dimples characteristic of quenched and tempered alloy steels.

Two-Stage, Plastic-Carbon Replica 14,000X



FIGURE 4. TENSILE FRACTURE OF Al-4.5% Cu (Alloy 2219) WELDMENT. Elongated, open dimples formed in shear lip of tensile test specimen. 5000X

Two-Stage, Plastic-Carbon Replica



FIGURE 5. IMPACT FRACTURE OF LOW-ALLOY STEEL (A302B). Tear dimples formed in Charpy Impact specimen broken at +5° F (103 ft.-lbs). Block arrow indicates macroscopic direction of crack propagation. Long arrow indicates local direction of crack propagation. 5000X

Two-Stage, Plastic-Carbon Replica

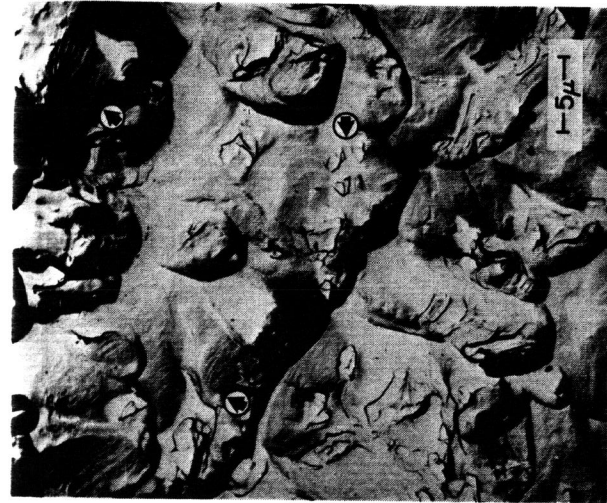


FIGURE 6. TENSILE FRACTURE OF Al-4.5% Cu (Alloy 2219) WELDMENT. Well defined ripples are evident on some dimple surfaces (oblique arrows). Stretching is indicated by separated parts of second-phase platelets (horizontal arrow). 5000X

Two-Stage, Plastic-Carbon Replica



FIGURE 7. TENSILE FRACTURE OF Al-4.5% Cu (Alloy 2219-T87). Note the range of dimple sizes. Arrows indicate origin of larger voids at second-phase platelets. 5000X

Two-Stage, Plastic-Carbon Replica

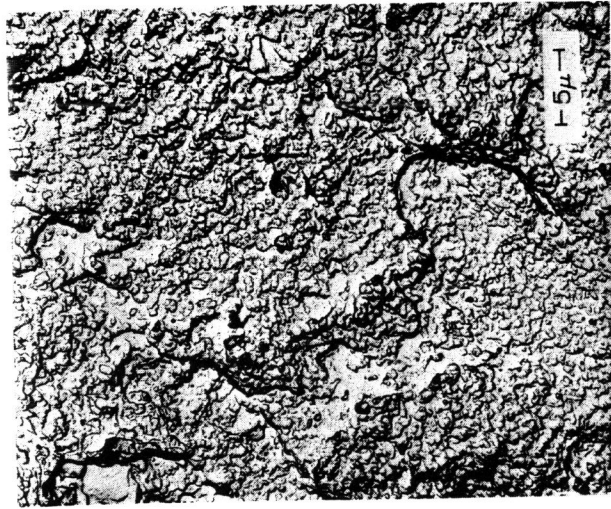


FIGURE 8. SURFACE TOPOGRAPHY OF BRITTLE FRACTURE IN Al-5.6% Zn (Alloy 7075-T6) FORGING. Small, uniform dimples typical of entire fracture surface of forging which failed in service. No measurable reduction in area was exhibited.

Two-Stage, Plastic-Carbon Replica

5000X

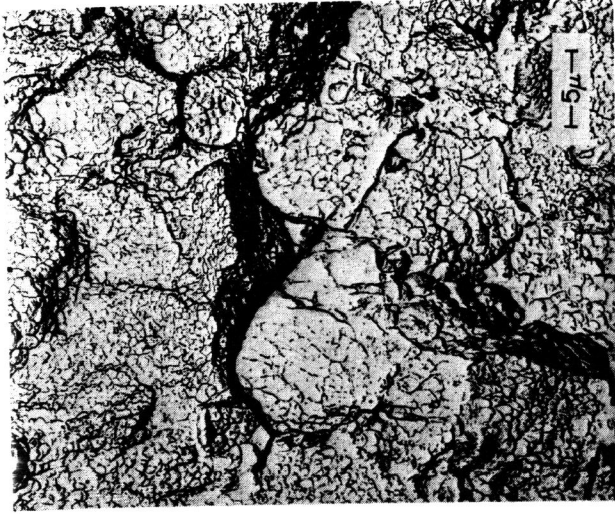


FIGURE 9. INTERGRANULAR FRACTURE IN Al-5.6% Zn (Alloy 7075-T6). Note small, uniform dimples superimposed on intergranular facets.

Two-Stage, Plastic-Carbon Replica

5000X

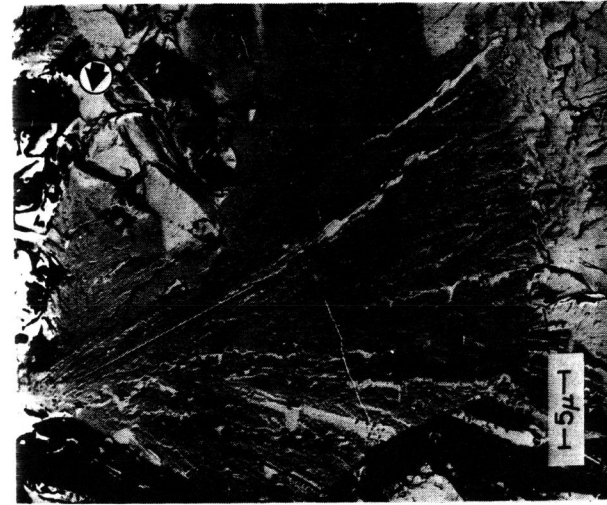


FIGURE 10. IMPACT FRACTURE OF LOW-ALLOY STEEL (A302B). Cleavage facet with well-defined steps and river patterns in Charpy impact specimen broken at -98° F (17 ft-lbs). Block arrow indicates macroscopic direction of crack propagation. Long arrow indicates local direction of crack propagation.

Two-Stage, Plastic-Carbon Replica

500X



FIGURE 11. IMPACT FRACTURE IN LOW-ALLOY STEEL (A302B). Cleavage facets in Charpy impact specimen broken at -98° F (17 ft-lbs). Horizontal arrows indicate narrow regions of deformed material separating cleavage facets. Block arrow indicates macroscopic direction of crack propagation. Long arrows indicate local directions of crack propagation.

Two-Stage, Plastic-Carbon Replica

2500X



FIGURE 12. IMPACT FRACTURE IN LOW-ALLOY STEEL (A302B). Mixed cleavage and microvoid coalescence in Charpy impact specimen broken at -60° F. Arrows indicate areas of small dimple formation.

Two-Stage, Plastic-Carbon Replica

5000X



FIGURE 13. IMPACT FRACTURE OF IRRADIATED LOW-ALLOY STEEL (A302B). Mixed cleavage and microvoid coalescence in Charpy impact specimen broken at +120° F (18 ft-lbs). Note the transition from cleavage to plastic fracture in the lower portion of the figure.

Two-Stage, Plastic-Carbon Replica

5000X



FIGURE 14. FATIGUE FRACTURE OF HIGH-STRENGTH STEEL. III-defined striations observed in service failure of quenched and tempered 4340 engine cylinder. Arrows indicate regions of post-fracture damage.

Two-Stage, Plastic-Carbon Replica

5000X

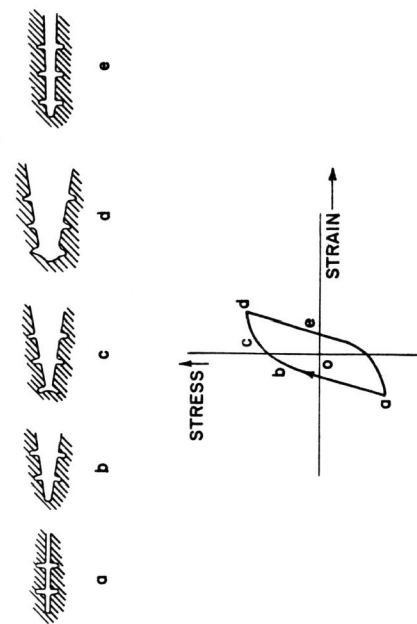


FIGURE 15. FATIGUE CRACK PROPAGATION SEQUENCE AS PROPOSED BY LAIRD AND SMITH. (25)

- (a) Crack tip sharpened at maximum compression part of cycle.
- (b) Crack opening as tensile part of cycle begins.
- (c) Extensive yielding and crack growth occur along planes of maximum shear of principal stress.
- (d) Deformation shifts to region along main crack plane.
- (e) Crack begins to sharpen as compression cycle begins.

STRIATION PROFILE - MATCHING SURFACES TYPE

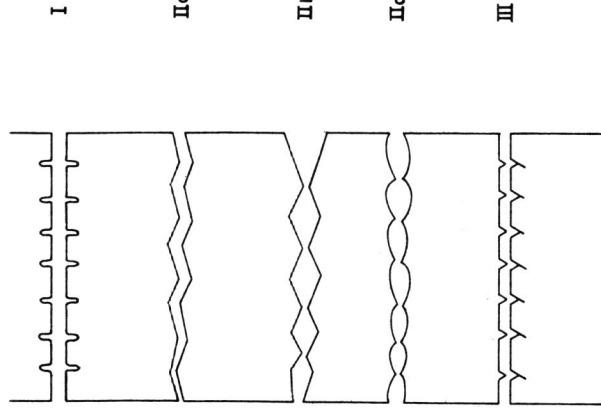


FIGURE 17. SUMMARY OF STRIATION PROFILE - MATCHING SURFACES.

- I - After Laird and Smith (23)
- II - After Forsyth(15), Stubbington (16), and Felloux(18)
- III - After Forsyth(15) and Stubbington (16)

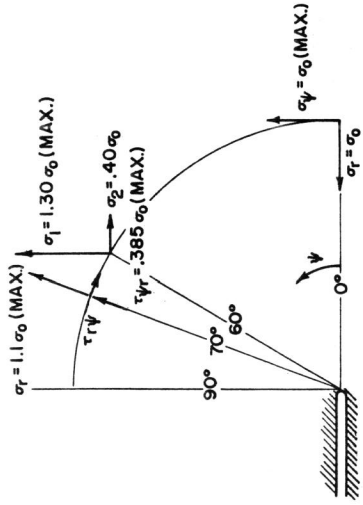


FIGURE 16. STRESS DISTRIBUTION AT THE BASE OF A STATIONARY CRACK. The maximums of tangential stress ( $\sigma_t$ ), radial stress ( $\sigma_r$ ), shear stress ( $\tau_{xy}$ ), and principal stress ( $\sigma_1$ ) are shown (after Williams 24).



FIGURE 18. HIGH-STRESS FATIGUE FRACTURE OF AUSTENITIC STAINLESS STEEL. Isolated dimples mixed with striations. Area near origin of crack. Failure occurred in 1786 cycles.

Two-Stage, Plastic-Carbon Replica

2500X



FIGURE 19. HIGH-STRESS FATIGUE FRACTURE OF AUSTENITIC STAINLESS STEEL. Same fracture of Figure 18, but from area further from crack origin. Note equiaxed, coalesced dimples.

Two-Stage, Plastic-Carbon Replica

5000X

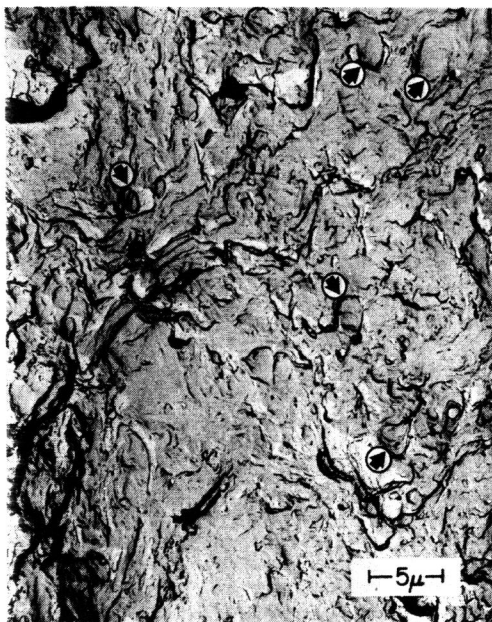


FIGURE 20. HIGH-STRESS FATIGUE FRACTURE OF LOW-ALLOY STEEL (A302B). Surface exhibits isolated dimples (arrows) and irregular surface markings.

Two-Stage, Plastic-Carbon Replica

5000X